16th World Conference on Earthquake Engineering, 16WCEE 2017
Santiago Chile, January 9th to 13th 2017
Paper N° 1037
Registration Code: S-F1462375462

PROBABILISTIC SEISMIC DAMAGE ASSESSMENT OF URM BUILDINGS BASED ON INCREMENTAL DYNAMIC ANALYSIS

J. A. Avila-Haro [(1)], R. González-Drigo [(2)], L. G. Pujades [(3)], A. Barbat [(3)]

[(1)] *Associate Professor; Dept. of Strength of Materials and Structural Engineering (EUETIB-CEIB), Technical University of Catalonia-BarcelonaTech (UPC); jorge.avia-haro@upc.edu*
[(2)] *Professor; Dept. of Strength of Materials and Structural Engineering (EUETIB-CEIB), Technical University of Catalonia-BarcelonaTech (UPC); jose.ramon.gonzalez@upc.edu*
[(3)] *Professor; Dept. of Civil and Environmental Engineering, Technical University of Catalonia-BarcelonaTech (UPC)*

Abstract

The main goal of this paper is to assess, from a probabilistic point of view, the seismic response of an unreinforced masonry building caused by the influence of the uncertainties and variability of the mechanical properties of the materials and the seismic actions. A seven-story isolated unreinforced masonry building is used as a case study. The typology to which the studied building corresponds is characterized by unidirectional iron beams-brick vaults slabs, supported by a system of solid clay brick load-bearing walls. Concerning the probabilistic assessment, the compressive strength (f_m), Young modulus (E), shear modulus (G) and shear strength (τ_0) of the solid clay masonry were considered as random variables. The damage assessment of the structure is inferred from the results obtained using the incremental dynamic analysis approach, which estimates the response of the structure when subjected to different levels of demand (*pga*) and a set of different ground motion records previously selected through the conditional spectrum method. The simple random sampling method without replacement was applied in order to obtain sufficiently representative samples for both, the values of the mechanical properties to be used, and the number of dynamic analyses to be performed. The results are categorized in accordance to the variables of interest. The response of the structure presents a visible tendency of higher values for the control variable, δ_{roof}, as the f_m values decrease and the *pga* values increase.

Keywords: probabilistic, mechanical properties, unreinforced masonry, conditional spectrum, incremental dynamic analysis

1. Introduction

Unreinforced masonry (URM) buildings belong to one of the most common and easily recognizable structural typologies of the urban dwelling stock of a large number of European cities. Despite the several similarities between these structure, many aspects, such as the year of construction, the construction methods, the quality of the labor force, the production processes and the quality of the materials, the intended use of the structure, or even the number of levels, determine their uniqueness in each country or region.

At present, this type of structures still represents a large proportion of nearly the 70% of the totality of 8 658 functional housing buildings of the City of Barcelona, Spain [1]. Furthermore, the majority of these buildings overpass 100 years old and were built without any consideration of the seismic action, making their study and subsequent assessment highly relevant in order to understand their vulnerability and response when subjected to any plausible solicitation.

The mechanical properties of the materials are one of the most common sources of epistemic uncertainties due to the extensive variability of the construction units (i.e., solid clay bricks), being of particular interest for the building typology analyzed in this work.

2. The Building

Since its very foundation as a roman colony, Barcelona was always considered a strategic military emplacement and an important commercial pole in the Mediterranean Basin. Its development and physical growth occurred in different stages along the time, experiencing several enlargements of its surrounding walls, which resulted only in temporary and insufficient solutions [2].

It was until 1856 when, without further limitations of the military ordinances, a complete and “unlimited” urban expansion of the city was allowed, including the demolition of the surrounding walls and the call for competition for the new enlargement (*Eixample* in catalan) project of the city [3, 4].

Among the different proposals, the project presented by the Civil Engineer Ildefonso Cerdà was selected and imposed by the central government. Nevertheless, and despite of being considered a watershed of the Urbanism of that age, the original project suffered distinct changes along the years in order to satisfy the demands of the different stakeholders and local authorities [5-7].

2.1 Main structural features

The selected URM building for this work is fully representative of the structural typology of the Eixample district, which mainly consists of unidirectional iron beams-brick vaults slabs, supported by a system of solid clay brick load-bearing walls. A detailed description of the structural and architectonic features of the analyzed URM building can be found in [8].

The ground floor level of this type of buildings consist of high ceilings (Fig. 1.c) and diaphanous areas used predominantly for hospitality business or commercial purposes (Fig. 1.a). The upper levels have lower heights and the presence of inner bearing and partition walls (Fig. 1.b), being used mostly for housing or, in a lesser percentage, for offices [9].

The load-bearing walls system is composed of the façades walls, the lateral (intermediate) walls between buildings and the inner courtyard. Metallic load-bearing columns and girders can be found in the ground floor level, which support the additional load-bearing walls of upper levels [8, 10].

The contribution of a secondary partition walls system is neglected since their thicknesses are lower than 10 cm and the contribution to the strength of the structure is not significant.

The elements of the different walls and floor systems are poorly or not connected at all among them. According to the span (Fig. 1.d), lintels and parapets of various materials and varying sizes are used above openings (doors, windows or balconies), which, being considerably weak areas, concentrate an important number of cracks and damages.

According to the council regulations and documents of the time [11, 12], a 350 kg/m^2 and a 200 kg/m^2 loads were considered as permanent and variable loads for the intermediate floors, respectively. A reduction on the variable load of 100 kg/m^2 was considered for the roof level.

The selection of the mortar and brick elements of the brickwork could vary depending on their quality, the type of structural element, range of loads to be resisted, height of the level, thickness of the wall, among other considerations.

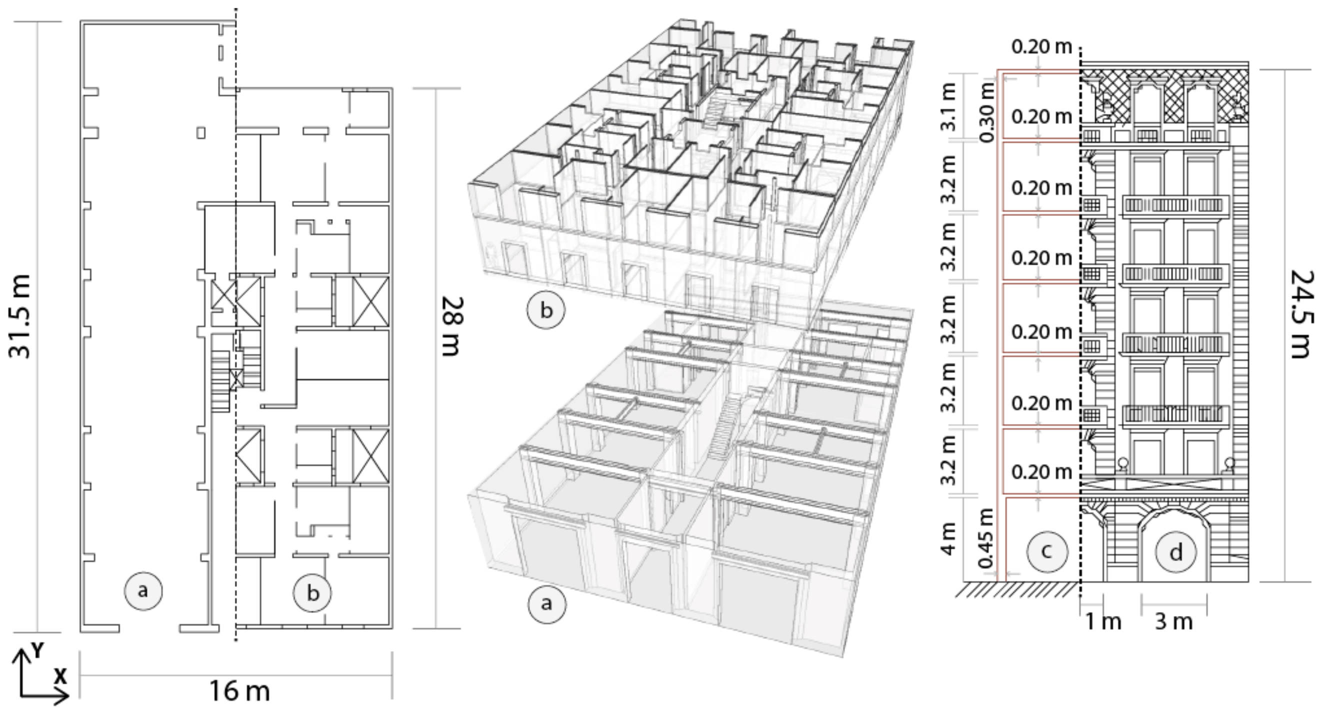

Fig. 1 Main structural distribution and dimensions: plan and isometric views of the ground (a) and typical (b) floors; and plan views of elevation (c) and front façade (d)

2.2 Computational model

The structure was modeled and analyzed through the Frame by Macro Element (FME) method, which is included in the 3MURI software and derives from the observation of the true behavior of buildings damaged by earthquakes taking into account the different damage mechanisms [13]. The software was developed by S.T.A. DATA in collaboration with the research teams from the universities of Genova and Pavia in Italy, led by prof. Sergio Lagomarsino [14-16].

As mentioned before, the main structural and architectural features of the building were modeled according to original floor plans, guidelines of the time, judgment of experts, technical and laboratory reports, as well as different databases. The model for this work considers only in-plane behavior of the walls, and a hysteretic law with a low-dissipation-level stiffness degrading (SD) and a softening parameter $\beta=0$.

3. Mechanical properties of the materials

The effects of all type of sources of epistemic uncertainties, described by means of random variables, can be taken into account in the probabilistic assessment of any structure. Nevertheless, the number, type and degree of influence of these uncertainties can significantly vary for each structure depending on different aspects such as the location, construction and production methods at the time, construction materials, building ordinances and codes, etc.

The construction period of the studied typology comprises the years 1860 to 1940 [1], in which the manufacturing of ceramic products intended for construction such as bricks, blocks, roofing or flooring tiles, was mainly done by hand with the use of local materials and rudimentary tools. Additionally, the firing process was performed in wood or coal-fired brick clamps or scove kilns, in which various factors such as the location of the pieces within the kiln, the lack of control over the firing once it started, or its susceptibility to external agents, produced scarce homogeneity and important fluctuations in the characteristics and quality of the finished product [17].

3.1 Variables of interest

The compressive strength (f_m), Young modulus (E), shear modulus (G) and shear strength (τ_0) of the solid clay masonry were considered as random variables. In addition, the range of values considered for f_m follow a two tailed normal distribution with α=10% and a confidence interval of 90%, whose corresponding critical values (i.e., rejection regions) closely resemble its previously established lower and upper bounds.

A hypothesis of positive linear correlation is assumed in the relationships between each variable and f_m: $E=E(f_m,\varepsilon)$; $G=G(E, \varepsilon)$ and $\tau_0=\tau_0(f_m, \varepsilon)$, where ε is a normally distributed variable with a zero mean value ($\mu_\varepsilon=0$) and a normalized variance ($var(\varepsilon)=1$), introduced in order to include the uncertainty of the hypothesized relationships. Additionally, with the purpose of adjusting the correlation in the distinct relationships and generating different samples of E, G and τ_0 in terms of f_m, a varying parameter is added, respectively.

Accordingly, the first relationship is:

$$E = 500 f_m + a\varepsilon \tag{1}$$

Where E, ε and f_m were previously defined, and a is the correlation adjustment varying parameter. In this relationship, the correlation coefficient between E and f_m is ρ:

$$\rho = \frac{cov\,(E, f_m)}{\sqrt{var(E) var(f_m)}} \tag{2}$$

Where $cov\,(E,f_m)$ is the covariance between E and f_m, and $var(E)$ and $var(f_m)$ are the variances of E and f_m, respectively.

For a given sample of f_m, the variance of E can be calculated as:

$$var(E) = var\,(500 f_m + a\varepsilon) = 500^2\, var(f_m) + a^2\, var(\varepsilon) \tag{3}$$

Moreover, the covariance between E and f_m can be easily calculated:

$$cov\,(E, f_m) = cov\,[(500 f_m + a\varepsilon),\, f_m] = 500\, var(f_m) + \, a \cdot cov(\varepsilon, f_m) = 500\, var(f_m) \tag{4}$$

Consequently, the correlation coefficient can be written in terms of the parameter a, and, by reversing the relationship, a can be expressed in terms of the coefficient of correlation ρ as:

$$a = \frac{500\sqrt{var(f_m)}}{\sqrt{var(\varepsilon)}} \sqrt{\frac{1}{\rho^2} - 1} \tag{5}$$

Following the same procedure undertaken previously for the Young modulus, the corresponding values for G and τ_0 can be generated based on the subsequent relationships:

$$G = \frac{1}{3} E + b\varepsilon \tag{6}$$

$$\tau_0 = 0{,}03 f_m + c\varepsilon \tag{7}$$

Where parameters b and c are used to adjust the correlations between G and E, and τ_0 and f_m, respectively.

3.2 Selected values

In order to extensively and sufficiently cover the possible variability, a total of N=1000 randomly generated and normally distributed units conform the finite population from which the sets of mechanical properties are generated according to the previously mentioned procedure. Suitable and reliable target values for each mechanical property of interest were determined based on the values and relationships reported in different sources [12, 18-25], numerous inspection visits and the opinion of experts.

The corresponding histograms and distribution functions of each variable, as well as the linear regression and correlation between each different pair of variables are presented in Fig. 2.

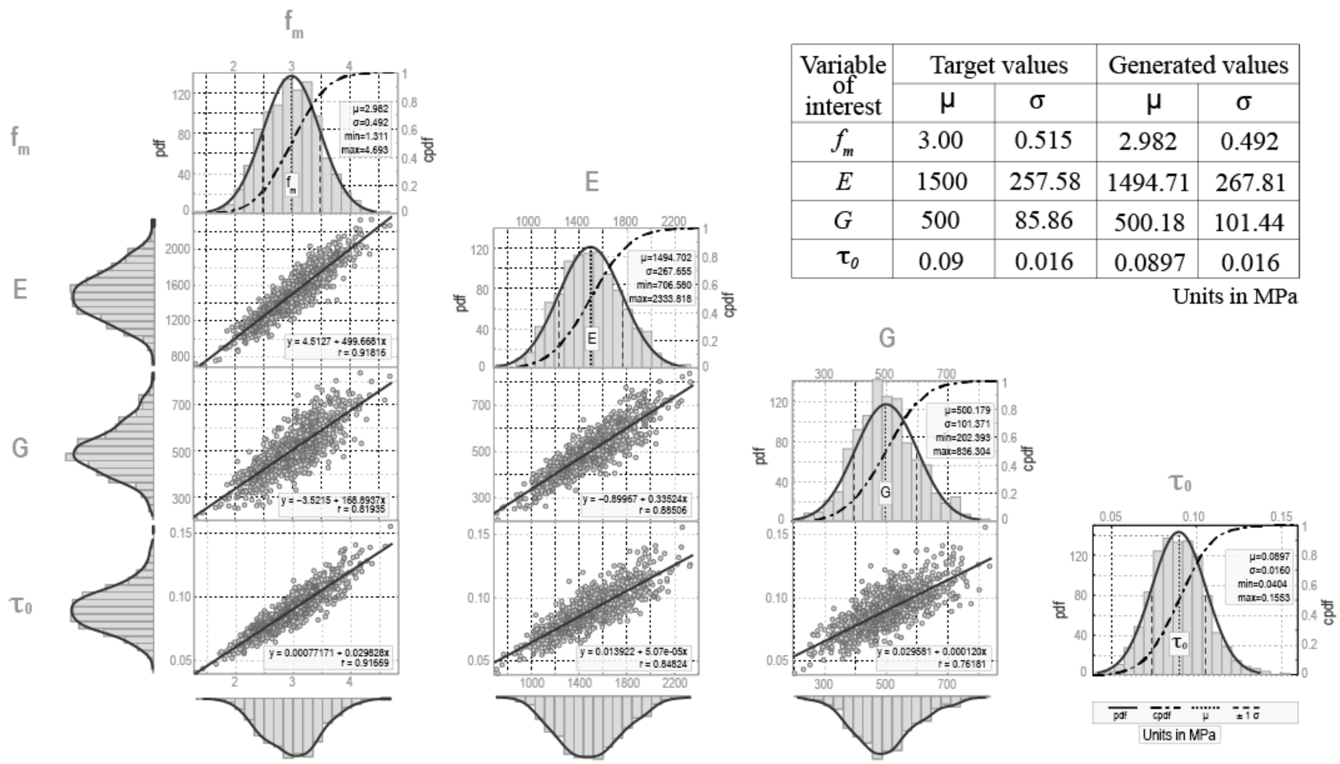

Variable of interest	Target values		Generated values	
	μ	σ	μ	σ
f_m	3.00	0.515	2.982	0.492
E	1500	257.58	1494.71	267.81
G	500	85.86	500.18	101.44
τ_0	0.09	0.016	0.0897	0.016

Units in MPa

Fig. 2 – Matrix of the mechanical properties sets for the analyzed population, including: (a) histogram and corresponding fitted and cumulative normal probability density functions for each mechanical property; and (b) linear regression and correlation coefficients of each combination of analyzed mechanical properties

4. Sampling

Different fields of science, mathematics, technology and engineering involve the study of large populations. Due to the nature and size of some of these populations, the survey of each unit composing them is impractical, unrealistic, and usually impossible. A more feasible approach consists in studying an appropriate and sufficiently representative sample of the population of interest, which allows to make statements or inferences with known accuracy about the whole, optimizing the workload and resources needed for this purpose.

For the purpose of this work, the simple random sampling (SRS) method without replacement was chosen. The SRS method considers that each unit of the population has an equal probability of being selected.

The calculation of the sample size, n, associated with the finite population, N, is performed assuming an equally skewed 50% sample proportion, p, a 5% margin of error and a 95% confidence level (α=5%), which are considered standard values in quantitative research (Eq. (8)). A finite population correction factor (FPC) was applied to take into account the fact that the sample is selected from a finite population without replacement and with a sampling fraction, n/N, greater than or equal to 5% (Eq. (9), Eq. (10) and Eq. (11)).

$$n_0 = \frac{\left(p \cdot (1-p)\right)}{\left({margin_{error}}/{z_{score}}\right)^2} \tag{8}$$

$$\sqrt{n} = \sqrt{n_0} \cdot FPC \tag{9}$$

$$FPC = \sqrt{{N-n}/{N-1}} \tag{10}$$

$$n = \frac{n_0 \cdot N}{(N-1) + n_0} \tag{11}$$

Where n_0 is the sample size without considering the FPC factor; and n is the corrected sample size to be used. A corrected sample size of n=278 is obtained for the finite population of N=1000 units of this work.

In order to verify that the selected sample for the compressive strength, f_m, comes from a normal distribution with population parameters μ=2.982 MPa and σ=0.492 MPa, a one-sample Kolmogorov-Smirnov test with a 5% significance level was performed.

5. Modal Analysis

As suggested in the literature, the number of degrees of freedom of the structure was condensed into three modes per floor (two horizontal translations and one rotation about the vertical). Consequently, and in order to consider that the number of computed modes is sufficient to capture the dynamic response of the structure, it was checked that the sum of the effective masses corresponding to the fundamental modes moved at least between 80% and 90% of the total mass for any given response direction. The latter, added to the corresponding box-behavior for this type of structures allowed to dismiss the influence of higher modes [26-29].

A total of 21 modes (GF+6 levels) were considered for each of the 278 selected samples in order to perform the modal analyses. For both directions, $+X$ and $+Y$, the percentage of activated mass in the first fundamental mode was considerably higher than in any other fundamental mode, confirming that the behavior of the structure is mainly governed by the first mode. The first natural periods for each direction, T_{1X}, T_{1Y}, and the resulting correlations with the different selected variables, f_m, E, G, and τ_0, are shown in Fig. 3.a.

6. Demand

Ten equal-size periods intervals were defined from the combined results (Eq. (12)) of the first fundamental periods for both directions, $+X$ and $+Y$ (Fig. 3.e).

$$T_{1XY} = \frac{(T_{1X} + T_{1Y})}{2} \tag{12}$$

As suggested in the literature [30-32], and for the average period of each interval, sets of 7 unscaled records were selected with the conditional spectrum (CS) method [33, 34] in order to match with the corresponding target design response spectrum (Fig. 4.a) for a probabilistic scenario, soil type 2 and pga=0.194g [35-37], obtained in accordance to the micro-zonation studies performed for the urban area of Barcelona and the location site of the building within the city [38-40].

It was observed that most of the records obtained for each interval were recurrent, and therefore a unique initial set of records was selected for all the periods intervals taking into account the ranking of the records previously obtained. In addition, a second record selection criterion was established due to certain software constrains regarding the number of points of the records and the complexity (number of nodes) of the computational model. Finally, after reducing significantly the number of points of each record through the Arias Intensity (AI) approach [41], a set of 7 representative records for all the periods intervals was selected (Fig. 4.b).

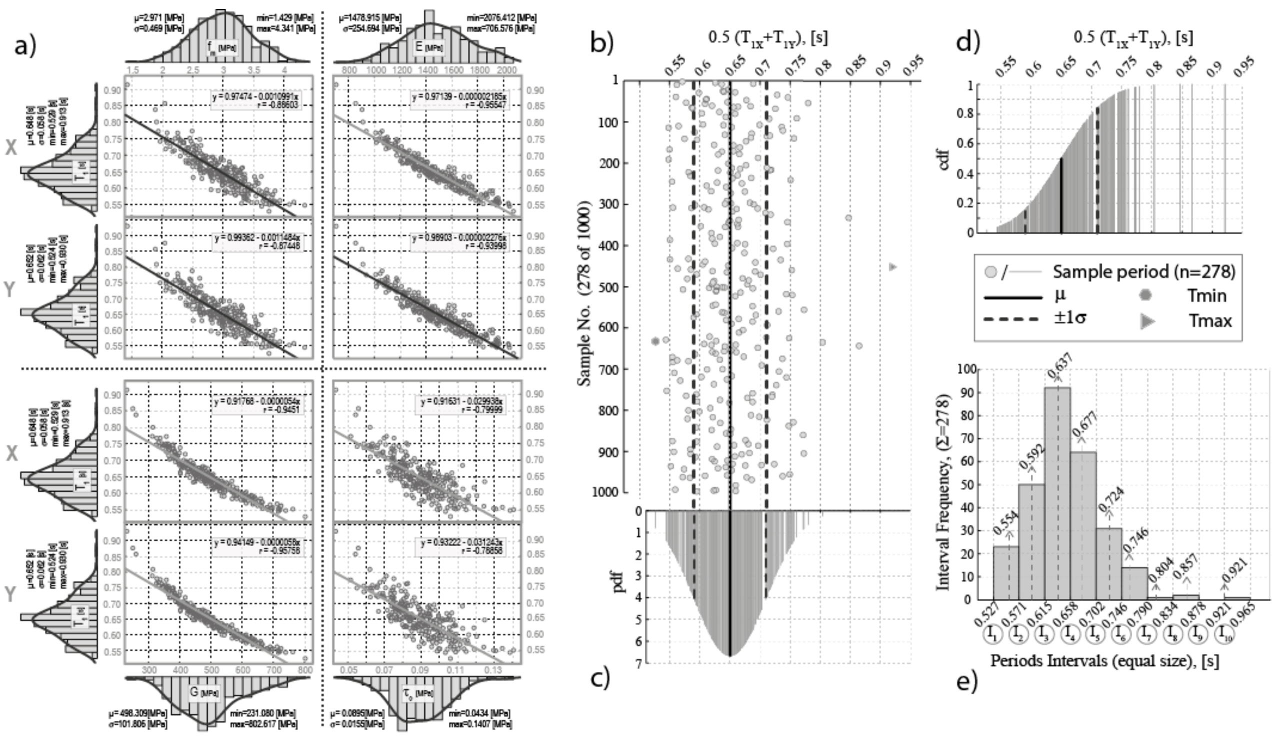

Fig. 3 – a) Correlation between the first fundamental vibration period, T_i, with the selected variables, f_m, E, G, and τ_0, for both analyzed directions, +X and +Y; b) combined first fundamental modes of both directions, T_{1X} and T_{1Y}; c) normal distribution function; d) cumulative distribution function; and e) equal-size periods intervals (histogram)

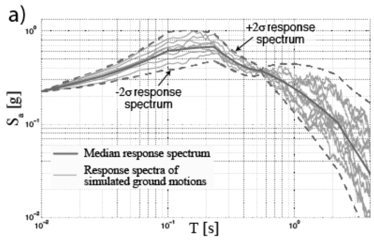

Record No.	Earthquake	Date (dd/mm/yy)	Time	Data Source	Station ID	PGA [g]
①	CHALFANT	07/31/86	07:22	CDMG	54171	0.119
②	HOLLISTER	01/26/86	19:20	USGS	1656	0.100
③	MANAGUA	12/23/72	07:19		3501	0.271
④	COALINGA	06/11/83	03:09	USGS	1606	0.191
⑤	HOLLISTER	01/26/86	19:20	USGS	1656	0.114
⑥	MAMMOTH	01/07/83	01:38	CDMG	54099	0.153
⑦	WHITTIER	10/04/87	10:59	CDMG	24400	0.261

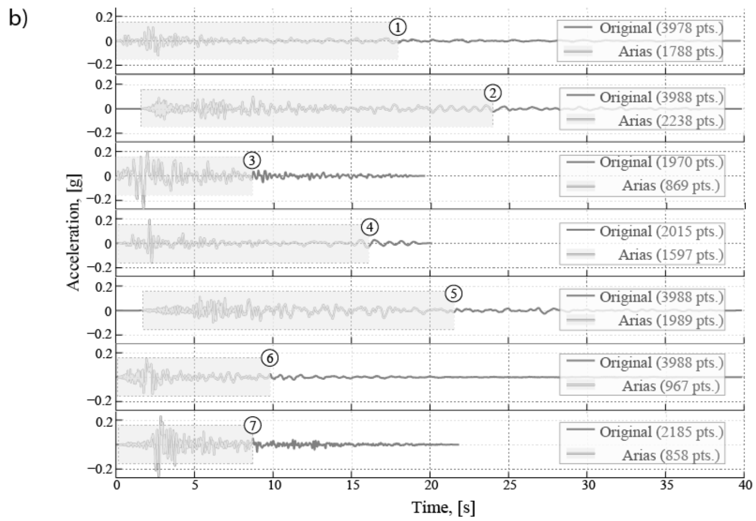

Fig. 4 – a) CS median response spectrum and records details; and b) Original and shortened (after AI) accelerograms of the selected records

7. Incremental Dynamic Analysis (IDA)

The incremental dynamic analysis (IDA) approach, proposed by Vamvatsikos and Cornell [42], takes into account the variability to which the structure is subjected by the use of one or more matching ground motion records, which are incrementally scaled to different *pga* values. Consequently, the procedure allows to estimate the evolution of the structural response of the building by means of a series of response curves in function of a control variable, (e.g. maximum roof displacement) in accordance with the incremental *pga* values used for each selected record. Despite the important computational effort and time consumption, this method is considered as a reference for the seismic risk evaluation.

For this work, the range of *pga* scaling values for the set of 7 records comprises the accelerations between 0.02 g and 0.30 g, with a Δpga of 0.01 g. Accordingly, the previously mechanical parameters sample (n=278), the number of records (7) and the number of scaling *pga* values (29) conform the second population, N_2=278x7x29=56 434 units, from which a sufficiently representative second sample, n_2=382, was selected following the sampling procedure explained in Section 4.

A total of 382 dynamic analyses were performed and post-processed for each direction with the 3MURI and MATLAB [43] programs, respectively.

Fig. 5 shows the corresponding results for all the 382 analysis for both directions of analysis, +*X* and +*Y*. It can be observed that as the PGA increases, the response of the structure increases as well. Nevertheless, the response can significantly fluctuate from one record to another due to specific particularities of each selected ground motion, such as the frequency content, the corresponding magnitude and *pga*, among others.

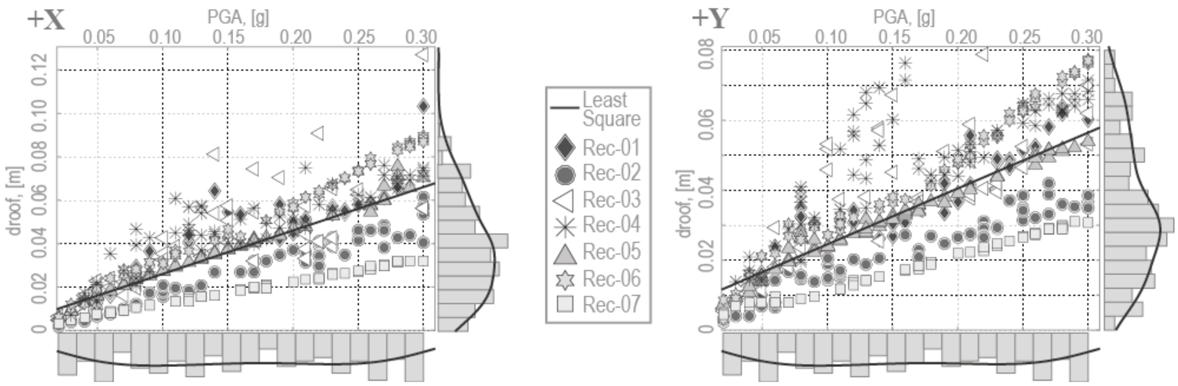

Fig. 5 IDA results for each sampled record and *pga*, for both directions, *+X* and *+Y*: PGA vs maximum roof displacement, δ_{roof}

The results are categorized and presented in accordance with the different variables of interest, f_m, E, G, and τ_0, either for each individual ground motion (Fig. 6) or for the full set of records (Fig. 7).

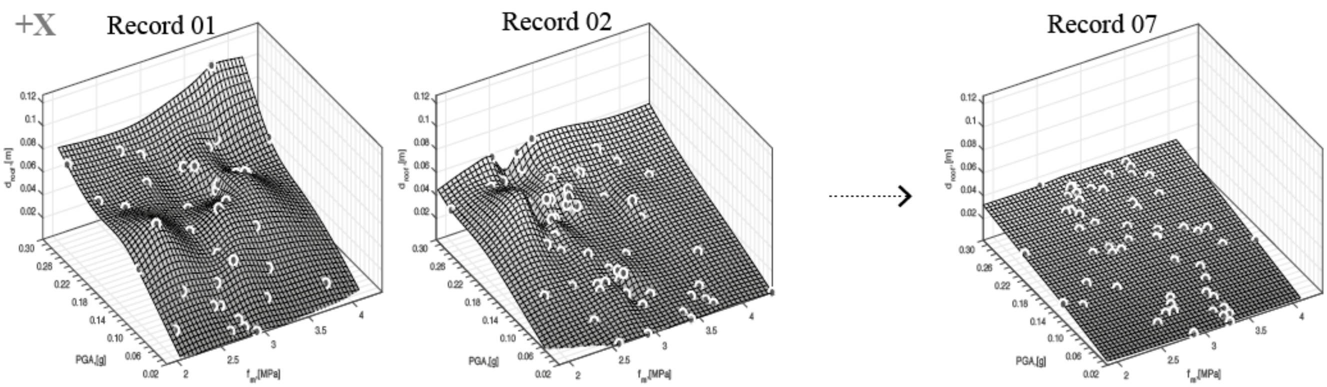

Fig. 6 Example of IDA results of the *+X* direction for f_m, with δ_{roof} as control variable for each individual sampled record and *pga*

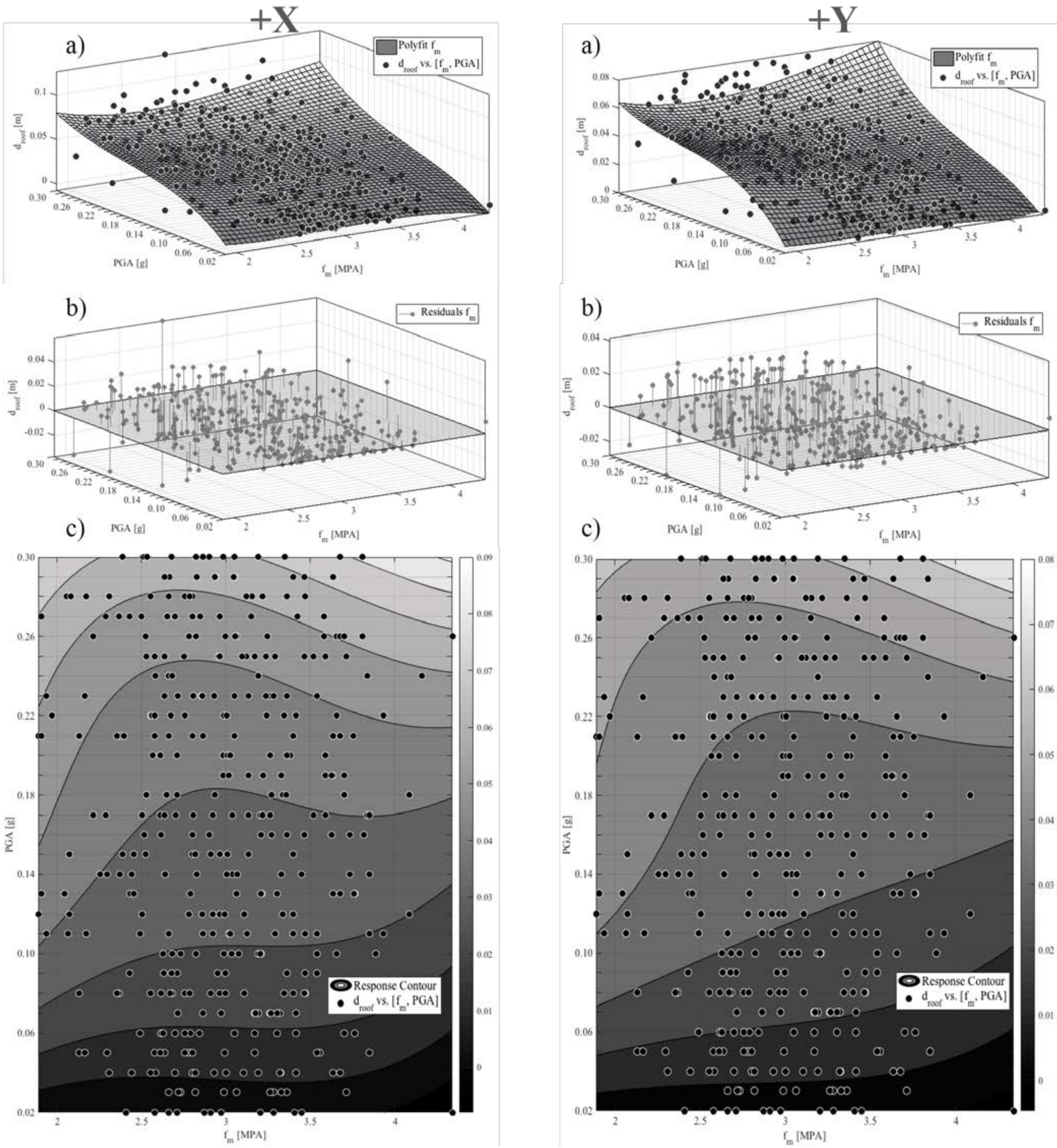

Fig. 7 IDA results for f_m, with δ_{roof} as control variable for the full set of selected records and values of *pga*: a) polyfit surface of the results; b) residuals plot; and c) contour plot

From the contour plots (Fig. 7.c) and for a specific *pga*, it can be observed that the response of the structure varies along the f_m values, presenting a visible tendency of higher displacements for lower f_m values as the *pga* increases.

The evolution of the control variable, δ_{roof}, with respect to the *pga* follows a lineal tendency with an adjusted slope which is lower for records 2 and 7, and higher for records 5 and 6, respectively. The difference in the slopes is considerable, since, for high *pga* values, the associated δ_{roof} of record 6 almost triples the corresponding δ_{roof} of record 2. Additionally, for records 3 and 4 the results presented in this work include a certain discontinuity in the response tendency in the form of high δ_{roof} values for intermediate *pga* values.

8. Conclusions

The results and the corresponding quality of any research study are significantly dependent on the selected sample(s). Therefore, an adequate, representative and properly designed sample is critical in order to prevent false or misleading results.

The dependence of the control variable, δ_{roof}, with respect to the *pga* is mainly lineal. Nevertheless, and depending on the selected record, it was observed that for high values of *pga*, the amplitude of the response differs considerably. This, along with the results for intermediate values of *pga* found for records 3 and 4, shows the need of a more detailed study for the selection of the records. For this work, the target design spectrum and the fundamental vibration period of the structure were taken into account as variables for the selection process. The inclusion of other parameters would permit a better adjustment.

A properly selected set of records permits to represent in an adequate form the variability of the demand, which is directly correlated with the obtained results. In order to reduce external/additional uncertainties and non-desirable effects, several parameters such as the frequency content, the *pga*, epicentral and hypocentral distances, focal depth, registered magnitude, record duration, among others, should be taken into account in this process.

The response of the structure presents a visible tendency of higher values for the control variable, δ_{roof}, as the f_m values decrease and the *pga* values increase.

Further future lines of research are advised taking into consideration other (extra) uncertainty sources such as live and dead loads, viscous damping, support length of lintels and slabs, wall thicknesses, sampling size, among others.

9. Acknowledgements

This research has been partially funded by the government of Spain (Ministry of Economy and Competitiveness –MINECO, in its Spanish acronym) and by the European Regional Development Fund (FEDER, in its Spanish acronym) of the European Union (EU) through projects referenced as: CGL2011-23621 and CGL2015-65913 -P (MINECO / FEDER, UE).

10. References

1. Lantada, N., *Aplicación de Técnicas GIS a Estimación de Riesgos Naturales*. 2007, Universitat Politècnica de Catalunya.
2. Sobrequés i Callicó, J., *Historia de Barcelona.*, ed. S.L. A & M Gràfics. 2008, Barcelona.
3. Permanyer, L., *Historia de L'Eixample.*, ed. P.y. Janés. 1990, Barcelona.
4. Permanyer, L., *L'Eixample. 150 Anys d'Historia*, ed. V. Edicions. 2011, Barcelona, Spain.
5. Ajuntament de Barcelona; Corporació Metropolitana de Barcelona, *Inicis de la Urbanística Municipal de Barcelona. Mostra dels Fons Municipals de Plans i Projectes d'Urbanisme 1750-1930*. 1985, Barcelona, Spain.
6. Busquets, J.R., *Barcelona. La construcción urbanística de una ciudad compacta*, ed. d. Serbal. 2004, Barcelona.
7. Busquets, J. and M. Corominas i Ayala, *Cerdà i la Barcelona del futur: realitat versus projecte*. 2009, Barcelona.
8. González-Drigo, R., et al., *Modernist URM buildings of Barcelona. Seismic Vulnerability and Risk Assessment.* International Journal of Architectural Heritage, 2015. **9**(3): p. 214-230.

9. Pujades, L., et al., *Seismic Performance of a Block of Buildings Representative of the Typical Construction in the Eixample District in Barcelona (Spain).* Bulletin of Earthquake Engineering, 2012(10): p. 331-349.
10. Paricio, A., *Secrets d'un Sistema Constructiu*. 2001, Barcelona, España: Edicions UPC.
11. Ministerio de la Vivienda, *Norma MV 101-1962. Acciones en la Edificación.*, in *Spanish Official Bulletin*. 1963, Ministerio de la Vivienda: Madrid, Spain.
12. Lahuerta, J. and L.F. Rodríguez, *Muros de Fábrica de Ladrillo. Normas y estudios extranjeros para su proyecto y ejecución*. 1962, Madrid: Ministerio de la Vivienda. Secretaría General Técnica.
13. S.T.A. DATA, *3muri Program*. 2012: http://www.3muri.com/.
14. Galasco, A., S. Lagomarsino, and A. Penna, *TREMURI Program: Seismic Analyser of 3D Masonry Building*. 2002: University of Genoa.
15. Lagomarsino, S., A. Galasco, and A. Penna, *Pushover and dynamic analysis of URM buildings by means of a non-linear macro-element model*, in *International Conference on Earthquake Loss Estimation and Risk Reduction*. 2002, RISK-UE project: Bucharest.
16. Lagomarsino, S., et al., *TREMURI program: An equivalent frame model for the nonlinear seismic analysis of masonry buildings.* Engineering Structures, 2013. **56**: p. 1787-1799.
17. Jones, T., *The Basics of Brick Kiln Technology*, in *Ein Titel von GATE,*. 1996, Vieweg & Sohn, Friedr.: Braunschweig/Wiesbaden, Germany.
18. PIET-70, *Obras de Fábrica*. 1971, Madrid: Instituto Eduardo Torroja.
19. CEAC, *Enciclopedia CEAC del Encargado de Obras. Materiales para la Construcción*. 1st ed, ed. CEAC. 1977, Barcelona: Ediciones CEAC.
20. Arredondo, F., *Estudio de Materiales. VI.-Cerámica y Vidrio*. 9th ed, ed. Consejo Superior de Investigaciones Científicas. 1980, Madrid: Instituto Eduardo Torroja de la Construcción y el Cemento.
21. Harris, H.A. *Masonry: Materials, Design, Construction and Maintenance*. in *Masonry: Materials, Design, Construction and Maintenance*. 1986. New Orleans, L.A.: American Society for Testing and Materials.
22. Hendry, A.W., B.P. Sinha, and S.R. Davies, *Design of Masonry Structures*. 3rd ed. 1987: E & FN Spon.
23. Hendry, A.W., *Structural Masonry*. 1990, Hong Kong: MacMillan Education LTD.
24. Drougkas, A., P. Roca, and C. Molins, *Numerical prediction of the behavior, strength and elasticity of masonry in compression.* Engineering Structures, 2015(90): p. 15-28.
25. Drougkas, A., P. Roca, and C. Molins, *Compressive strength and elasticity of pure lime mortar masonry.* Materials and Structures, 2016(49): p. 983-999.
26. Barbat, A., *Cálculo sísmico de estructuras*. 1982, Barcelona: Editores Técnicos Asociados.
27. Priestley, M.J.N., F. Seible, and G.M. Calvi, *Seismic Design and Retrofit of Bridges*. 1996, New York: John Wiley and Sons.
28. Barbat, A., S. Oller, and J.C. Vielma, *Cálculo y diseño sismorresistente de edificios: aplicación de la norma NCSE-02,*, in *Monografías de Ingeniería Sísmica,*, A. Barbat, Editor. 2005, Centro Internacional de Métodos Numéricos en Ingeniería,: Barcelona, España.
29. Fardis, M.N., *Seismic Design, Assessment and Retrofitting of Concrete Buidings based on EN-Eurocode 8*. Geotechnical, Geological, and Earthquake Engineering, ed. A. Ansal. 2009, New York: Springer.
30. Bommer, J. and C. Ruggeri, *The specification of acceleration time-histories in seismic design codes.* European Earthquake Engineering, 2002. **16**(1): p. 3-17.
31. Eurocode-8-1, *Design of Structures for Earthquake Resistance. Part 1: General Rules, Seismic Actions and Rules for Buildings*. 2004, Comité Européen de Normalisation.
32. Hancock, J., J. Bommer, and P.J. Stafford, *Numbers of scaled and matched accelerograms required for inelastic dynamic analysis.* Earthquake Engineering and Structural Dynamics, 2008. **37**: p. 1585-1607.
33. Baker, J.W., et al., *New Ground Motion Selection Procedures and Selected Motions for the PEER Transportation Research Program*. 2011, PEER Technical Report 2011/03. p. 106.
34. Jayaram, N., T. Lin, and J.W. Baker, *A Computationally Efficient Ground Motion Selection Algorithm for Matching a Target Response Spectrum Mean and Variance.* Earthquake Spectra, 2011. **27**(3): p. 797-815.

35. Irizarry, J., X. Goula, and T. Susagna, *Analytical Formulation for the Elastic Acceleration-Displacement Response Spectra Adapted to Barcelona Soil Conditions*. 2003, Institut Cartogràfic de Catalunya: Barcelona, Spain.
36. Irizarry, J., *An Advanced Approach to Seismic Risk Assessment. Application to the Cultural Heritage and the Urban System of Barcelona*. 2004, Universitat Politècnica de Catalunya, UPC: Barcelona, Spain. p. 406.
37. Irizarry, J., et al., *Ground-shaking scenarios and urban risk evaluation of Barcelona using the Risk-UE capacity spectrum method.* Bulletin of Earthquake Engineering, 2011. **9**: p. 441-446.
38. Cid, J., *Zonación sísmica de la ciudad de Barcelona basada en métodos de simulación numérica de efectos locales*. 1998, Universitat Politècnica de Catalunya, UPC: Barcelona, Spain. p. 215.
39. Secanell, R., et al. *Analysis of Seismic Hazard in Catalonia (Spain) through Different Probabilistic Approaches*. in *Proceedings of the 11th European Conference on Earthquake Engineering*. 1998. Paris, France: Balkema.
40. Secanell, R., et al., *Seismic hazard zonation of Catalonia, Spain, integrating uncertainties.* Journal of Seismology, 2004. **8**: p. 24–40.
41. Arias, A., *A measure of earthquake intensity*, in *Seismic Design of Nuclear Power Plants*, R. Hansen, Editor. 1970, MIT Press: Cambridge, MA. p. 438-483.
42. Vamvatsikos, D. and C.A. Cornell, *Incremental Dynamic Analysis.* Earthquake Engineering and Structural Dynamics, 2002. **31**(3): p. 491-514.
43. The MathWorks, I., *MATLAB Release 2009b* 2009b: Massachusetts, United States.